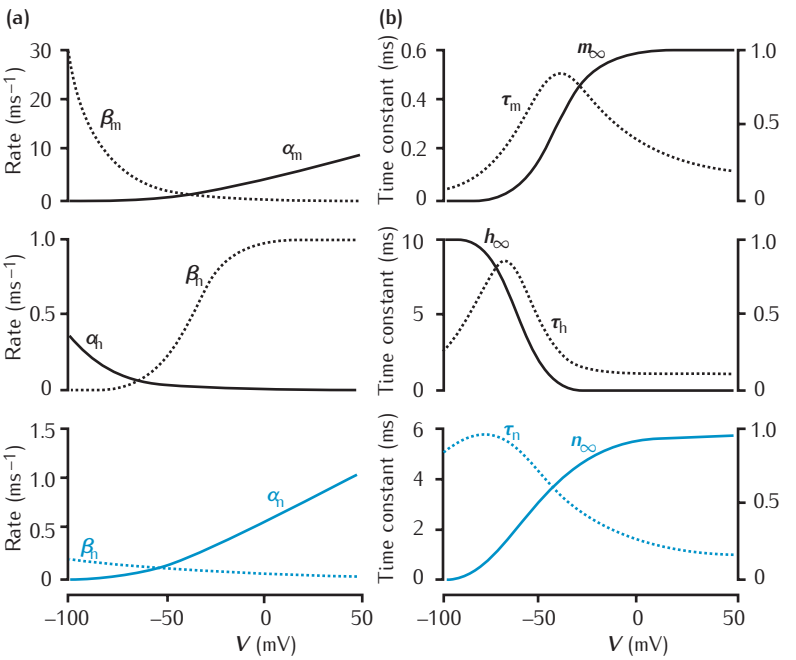

Fig. 3.10 Voltage dependence of rate coefficients and limiting values and time constants for the Hodgkin–Huxley gating variables. **(a)** Graphs of forward rate variables α_m, α_h and α_n (solid lines) and backward rate variables β_m, β_h and β_n (dashed lines) for the m, h and n gating particles. **(b)** The equivalent graphs for m_∞, h_∞ and n_∞ (solid lines) and τ_m, τ_h and τ_n (dotted lines).

3.3 Simulating action potentials

In order to predict how the membrane potential changes over time, the complete system of coupled non-linear differential equations comprising the HH model (Box 3.5) have to be solved. Hodgkin and Huxley used numerical integration methods (Appendix B.1). It took them three weeks' work on a hand-operated calculator. Nowadays, it takes a matter of milliseconds for fast computers to solve the many coupled differential equations in a compartmental formulation of the HH model.

In this section we look at the action potentials that these equations predict, both under space clamp conditions and under free propagation conditions. This will lead us to comparisons with experimental recordings and a brief review of the insights that this model provided. It is worth noting that the recordings in this section were all made at 6.3 °C, and the equations and simulations all apply to this temperature. Hodgkin and Huxley discovered that temperature has a strong influence on the rate coefficients of the gating variables, but were able to correct for this, as will be discussed in Section 3.4.

3.3.1 Space clamped action potentials

In one set of experiments under space clamp (but not voltage clamp) conditions, Hodgkin and Huxley depolarised the membrane potential to varying levels by charging the membrane quickly with a brief current clamp pulse. Small depolarisations led to the membrane potential decaying back to its resting value, but when the membrane was depolarised above a threshold of around 10 mV above resting potential, action potentials were initiated

Box 3.5 Summary of the Hodgkin–Huxley model

The equation for the membrane current is derived by summing up the various currents in the membrane, including spatial spread of current from local circuits:

$$C_m \frac{\partial V}{\partial t} = -\bar{g}_L(V - E_L) - \bar{g}_{Na} m^3 h (V - E_{Na}) - \bar{g}_K n^4 (V - E_K) + \frac{d}{4R_a} \frac{\partial^2 V}{\partial x^2}.$$

Under space clamp conditions, i.e. no axial current:

$$C_m \frac{dV}{dt} = -\bar{g}_L(V - E_L) - \bar{g}_{Na} m^3 h (V - E_{Na}) - \bar{g}_K n^4 (V - E_K).$$

Sodium activation and inactivation gating variables:

$$\frac{dm}{dt} = \alpha_m(1 - m) - \beta_m m, \qquad \frac{dh}{dt} = \alpha_h(1 - h) - \beta_h h,$$

$$\alpha_m = 0.1 \frac{V + 40}{1 - \exp(-(V + 40)/10)}, \qquad \alpha_h = 0.07 \exp(-(V + 65)/20),$$

$$\beta_m = 4 \exp(-(V + 65)/18), \qquad \beta_h = \frac{1}{\exp(-(V + 35)/10) + 1}.$$

Potassium activation gating variable:

$$\frac{dn}{dt} = \alpha_n(1 - n) - \beta_n n,$$

$$\alpha_n = 0.01 \frac{V + 55}{1 - \exp(-(V + 55)/10)},$$

$$\beta_n = 0.125 \exp(-(V + 65)/80).$$

Parameter values (from Hodgkin and Huxley, 1952d):

$C_m = 1.0\ \mu F\,cm^{-2}$

$E_{Na} = 50\ mV$ $\qquad \bar{g}_{Na} = 120\ mS\,cm^{-2}$

$E_K = -77\ mV$ $\qquad \bar{g}_K = 36\ mS\,cm^{-2}$

$E_L = -54.4\ mV$ $\qquad \bar{g}_L = 0.3\ mS\,cm^{-2}$

See Figure 3.10 for plots of the voltage dependence of the gating particle rate coefficients.

(Figure 3.11). Hodgkin and Huxley referred to these action potentials induced under space clamp conditions as **membrane action potentials**.

To simulate the different depolarisations in experiments, they integrated the equations of their space clamped model with different initial conditions for the membrane potential. Because the current pulse that caused the initial depolarisation was short, it was safe to assume that initially n, m and h were at their resting levels.

The numerical solutions were remarkably similar to the experimental results (Figure 3.11). Just as in the experimental recordings, super-threshold depolarisations led to action potentials and sub-threshold ones did not, though the threshold depolarisation was about 6 mV above rest instead of 10 mV. The time courses of the observed and calculated action potentials were very similar, although the peaks of the calculated action potentials were too sharp and there was a kink in the falling part of the action potential curve.

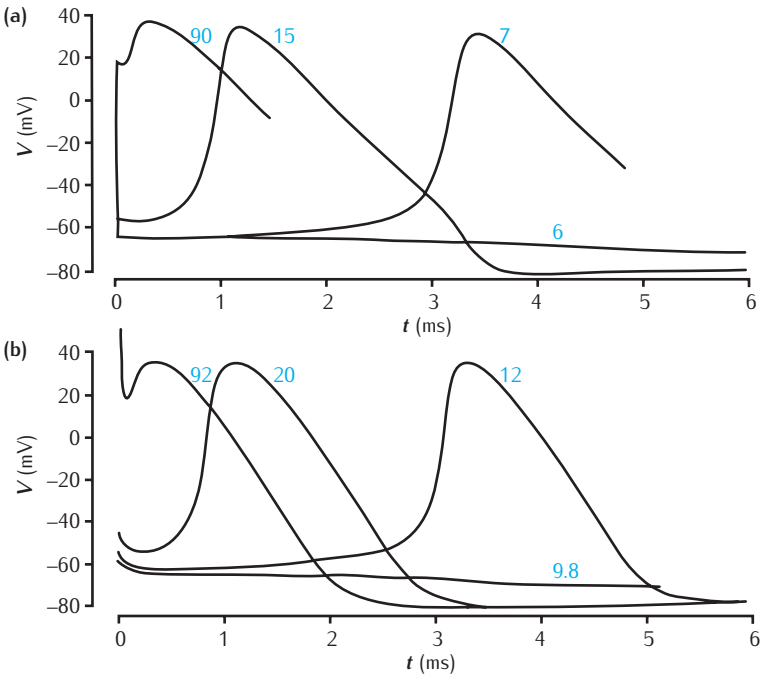

Fig. 3.11 Simulated and experimental membrane action potentials. **(a)** Solutions of the Hodgkin–Huxley equations for isopotential membrane for initial depolarisations of 90, 15, 7 and 6 mV above resting potential at 6.3 °C. **(b)** Experimental recordings with a similar set of initial depolarisations at 6.3 °C. Adapted from Hodgkin and Huxley (1952d), with permission from John Wiley & Sons Ltd.

Besides reproducing the action potential, the HH model offers insights into the mechanisms underlying it, which experiments alone were not able to do. Figure 3.12 shows how the sodium and potassium conductances and the gating variables change during a membrane action potential. At the start of the recording, the membrane has been depolarised to above the threshold. This causes activation of the sodium current, as reflected in the increase in m and g_{Na}. Recall that the dependence of m on the membrane potential is roughly sigmoidal (Figure 3.10). As the membrane potential reaches the sharply rising part of this sigmoid curve, the g_{Na} activation increases greatly. As the sodium reversal potential is much higher than the resting potential, the voltage increases further, causing the sodium conductance to increase still further. This snowball effect produces a sharp rise in the membrane potential.

The slower potassium conductance g_K, the n gating variable, starts to activate soon after the sharp depolarisation of the membrane. The potassium conductance allows current to flow out of the neuron because of the low potassium reversal potential. The outward current flow starts to repolarise the cell, taking the membrane potential back down towards rest. It is the delay in its activation and repolarising action that leads to this type of potassium current being referred to as the **delayed rectifier** current.

The repolarisation of the membrane is also assisted by the inactivating sodium variable h, which decreases as the membrane depolarises, causing the inactivation of g_{Na} and reduction of the sodium current flow into the cell. The membrane potential quickly swoops back down to its resting level, overshooting somewhat to hyperpolarise the neuron. This causes the rapid deactivation of the sodium current (m reduces) and its **deinactivation**,

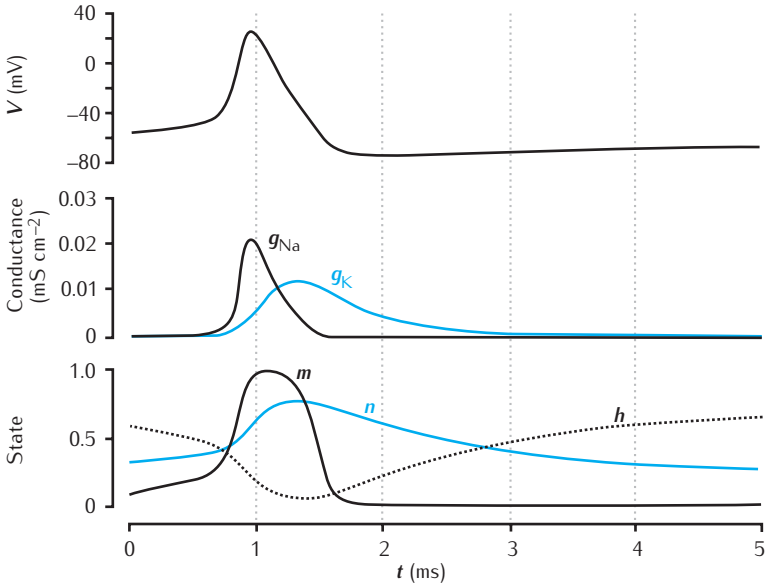

Fig. 3.12 The time courses of membrane potential, conductances and gating variables during an action potential.

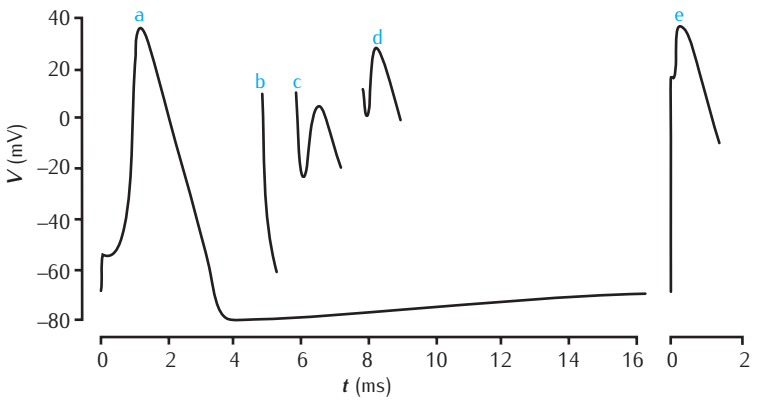

Fig. 3.13 Refractory properties of the HH model. Upper curves are calculated membrane action potentials at 6.3 °C. Curve a is the response to a fast current pulse that delivers 15 nC cm^{-2}. Curves b to d are the responses to a charge of 90 nC cm^{-2} delivered at different times after the initial pulse. Adapted from Hodgkin and Huxley (1952d), with permission from John Wiley & Sons Ltd.

whereby the inactivation is released (h increases). In this phase, the potassium conductance also deactivates. Eventually all the state variables return to their resting states and the membrane potential returns to its resting level.

The HH model also explains the **refractory period** of the axon. During the **absolute refractory period** after an action potential, it is impossible to generate a new action potential by injecting current. Thereafter, during the **relative refractory period**, the threshold is higher than when the membrane is at rest, and action potentials initiated in this period have a lower peak voltage. From Figure 3.12, the gating variables take a long time, relative to the duration of an action potential, to recover to their resting values. It should be harder to generate an action potential during this period for two reasons. Firstly, the inactivation of the sodium conductance (low value of h) means that any increase in m due to increasing voltage will not increase the sodium conductance as much as it would when h is at its higher resting value

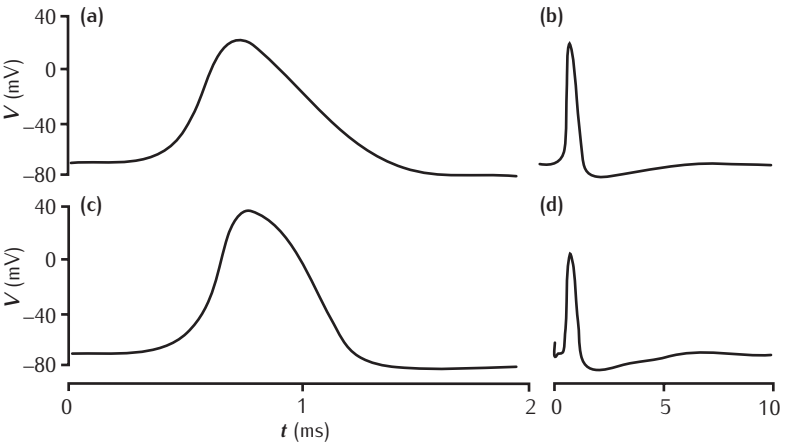

Fig. 3.14 Calculated and recorded propagating action potentials. **(a)** Time course of action potential calculated from the Hodgkin–Huxley equations. The conduction velocity was 18.8 m s^{-1} and the temperature 18.5 °C. **(b)** Same action potential at a slower timescale. **(c)** Action potential recorded from squid giant axon at 18.5 °C on same time scale as simulation in **(a)**. **(d)** Action potential recorded from a different squid giant axon at 19.2 °C at a slower timescale. Adapted from Hodgkin and Huxley (1952d), with permission from John Wiley & Sons Ltd.

(Figure 3.10). Secondly, the prolonged activation of the potassium conductance means that any inward sodium current has to counteract a more considerable outward potassium current than in the resting state. Hodgkin and Huxley's simulations (Figure 3.13) confirmed this view, and were in broad agreement with their experiments.

Hodgkin and Huxley had to assume that the membrane potential propagated at a constant velocity so that they could convert the partial differential equation into a second order ordinary differential equation, giving a soluble set of equations.

3.3.2 Propagating action potentials

The propagated action potential calculated by Hodgkin and Huxley was also remarkably similar to the experimentally recorded action potential (Figure 3.14). The value of the velocity they calculated was 18.8 m s^{-1}, close to the experimental value of 21.2 m s^{-1} at 18.5 °C.

Figure 3.15 shows the capacitive, local and ionic currents flowing at different points on the membrane at a particular instant when an action potential is propagating from left to right. At the far right, local circuit currents are flowing in from the left because of the greater membrane potential there. These local circuit currents charge the membrane capacitance, leading to a rise in the membrane potential. Further to the left, the membrane is sufficiently depolarised to open sodium channels, allowing sodium ions to flow into the cell. Further left still, the sodium ionic current makes a dominant contribution to charging the membrane, leading to the opening of more sodium channels and the rapid rise in the membrane potential that characterises the initial phase of the action potential. To the left of this, the potassium conductance is activated, due to the prolonged depolarisation. Although sodium ions are flowing into the cell here, the net ionic current is outward. This outward current, along with a small local circuit contribution, discharges the membrane capacitance, leading to a decrease in the membrane potential. At the far left, in the falling part of the action potential, only potassium flows as sodium channels have inactivated. The final **afterhyperpolarisation** potential is not shown fully for reasons of space and because the current is very small. In this part, sodium is deinactivating and potassium is deactivating. This leads to a small inward current that brings the membrane potential back up to its resting potential.

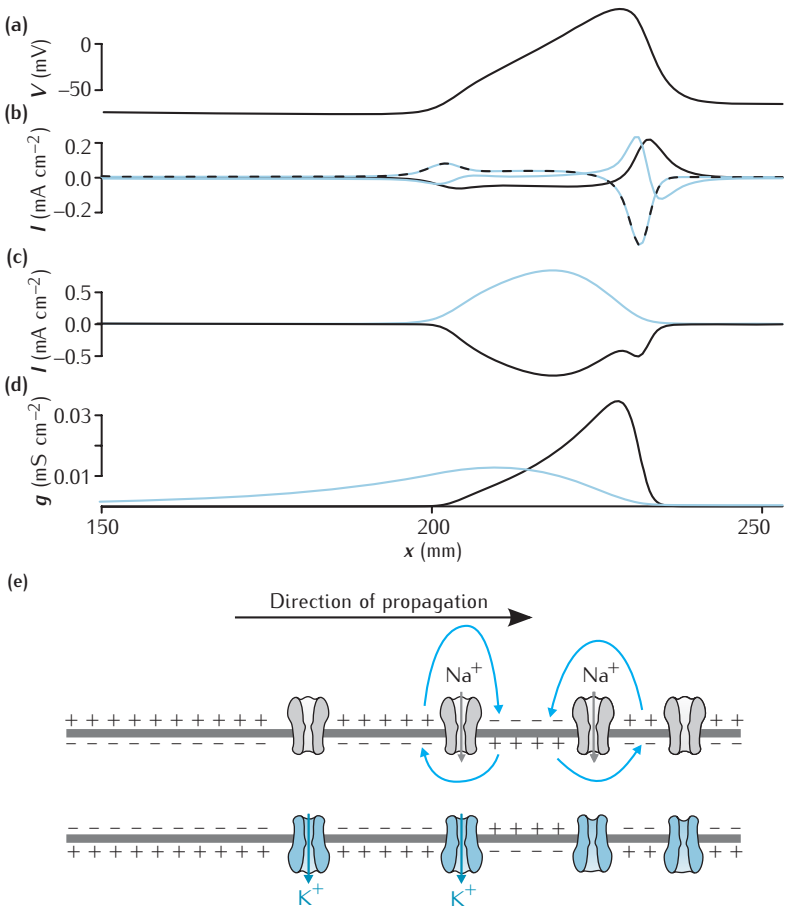

Fig. 3.15 Currents flowing during a propagating action potential. **(a)** The voltage along an axon at one instant in time during a propagating action potential. **(b)** The axial current (blue line), the ionic current (dashed black–blue line) and the capacitive current (black line) at the same points. **(c)** The sodium (black) and potassium (blue) contributions to the ionic current. The leak current is not shown. **(d)** The sodium (black) and potassium (blue) conductances. **(e)** Representation of the state of ion channels, the membrane and local circuit current along the axon during a propagating action potential.

3.4 The effect of temperature

Hodgkin *et al.* (1952) found that the temperature of the preparation affects the time course of voltage clamp recordings strongly: the rates of activation and inactivation increase with increasing temperature. In common with many biological and chemical processes, the rates increase roughly exponentially with the temperature. The Q_{10} **temperature coefficient**, a measure of the increase in rate for a 10 °C temperature change, is used to quantify this temperature dependence:

$$Q_{10} = \frac{\text{rate at } T + 10\,^{\circ}\text{C}}{\text{rate at } T}. \tag{3.21}$$

If the values of the HH voltage-dependent rate coefficients α and β at a temperature T_1 are $\alpha(V, T_1)$ and $\beta(V, T_1)$, then their values at a second temperature T_2 are:

$$\alpha(V, T_2) = \alpha(V, T_1) Q_{10}^{\frac{T_2 - T_1}{10}} \quad \text{and} \quad \beta(V, T_2) = \beta(V, T_1) Q_{10}^{\frac{T_2 - T_1}{10}}. \tag{3.22}$$

In the alternative form of the kinetic equations for the gating variables (see, for example, Equation 3.11), this adjustment due to temperature can

be achieved by decreasing the time constants τ_n, τ_m and τ_h by a factor of $Q_{10}^{(T_2-T_1)/10}$ and leaving the steady state values of the gating variables n_∞, m_∞ and h_∞ unchanged.

Hodgkin *et al.* (1952) estimated, from recordings, a Q_{10} of about 3 for the time constants of the ionic currents. This is typical for the rate coefficients of ion channels (Hille, 2001). In fact, the principles of transition state theory, outlined in Section 5.8.1, show that the Q_{10} itself is expected to depend on temperature: the Q_{10} at 6 °C is not expected to be the same as the Q_{10} measured at 36 °C. Transition state theory also allows temperature to be incorporated into the equations for the rate coefficients explicitly, rather than as a correction factor.

Assuming that reaction rate increases exponentially with temperature is equivalent to assuming that the effect is multiplicative. If the rate coefficient increases by a factor Q for a 1 °C increase in temperature, for a 2 °C increase it is $Q \times Q$; for a 10 °C increase it is $Q_{10} \equiv Q^{10}$ and for an increase from T_1 to T_2 it is $Q^{(T_2-T_1)}$ or $Q_{10}^{(T_2-T_1)/10}$.

As well as the rate coefficients, the maximum channel conductances also increase with temperature, albeit not as strongly. If the maximum conductance for an ion type X is $\overline{g}_X(T_1)$ at temperature T_1, at temperature T_2 it will be given by:

$$\overline{g}_X(T_2) = \overline{g}_X(T_1) Q_{10}^{\frac{T_2-T_1}{10}}. \tag{3.23}$$

The Q_{10} is typically around 1.2 to 1.5 for conductances (Hodgkin *et al.*, 1952; Rodriguez *et al.*, 1998; Hille, 2001).

3.5 Building models using the Hodgkin–Huxley formalism

The set of equations that make up the HH model (Box 3.5) were constructed to explain the generation and propagation of action potentials specifically in the squid giant axon. How relevant is the HH model to other preparations? While the parameters and equations for the rate coefficients present in the HH model are particular to squid giant axon, the general idea of gates comprising independent gating particles is used widely to describe other types of channel. In this section, we explore the model assumptions and highlight the constraints imposed by the Hodgkin–Huxley formalism. Moreover, we outline the types of experimental data that are required in order to construct this type of model of ion channels.

3.5.1 Model approximations

The HH model contains a number of approximations of what is now known about the behaviour of channels. Each of these will induce an error in the model, but the approximations are not so gross as to destroy the explanatory power of the model.

Each channel type is permeable to only one type of ion

Implicit in the HH model is the notion that channels are selective for only one type of ion. In fact, all ion channels are somewhat permeable to ions other than the dominant permeant ion (Section 2.1). Voltage-gated sodium channels in squid giant axon are about 8% as permeable to potassium as they are to sodium, and potassium channels are typically around 1% as permeable to sodium as they are to potassium (Hille, 2001).

The independence principle

As it is assumed that each type of current does not depend on the concentrations of other types of ion, these equations imply that the independence principle holds (Box 2.4). Hodgkin and Huxley (1952a) verified, to the limit of the resolving power of their experiments, that the independence principle holds for the sodium current. However, improved experimental techniques have revealed that this principle of independence does not hold exactly in general (Section 2.7).

The linear instantaneous *I–V* characteristic

One of the key elements of the HH model is that all the ionic currents that flow though open gates have a linear, quasi-ohmic dependence on the membrane potential (Equations 3.3–3.5), for example:

$$I_{\mathrm{Na}} = g_{\mathrm{Na}}(V - E_{\mathrm{Na}}). \tag{3.3}$$

As described in Chapter 2, this relation is an approximation of the non-linear Goldman–Hodgkin–Katz current equation, which itself is derived theoretically from assumptions such as there being a constant electric field in the membrane.

Hodgkin and Huxley (1952b) did not take these assumptions for granted, and carried out experiments to check the validity of Equation 3.3, and the corresponding equation for potassium. Testing this relation appears to be a matter of measuring an *I–V* characteristic, but in fact it is more complicated, since, as seen earlier in the chapter, the conductance g_{Na} changes over time, and the desired measurements are values of current and voltage at a *fixed* value of the conductance. It was not possible for Hodgkin and Huxley to fix the conductance, but they made use of their observation that it is *rate of change* of an ionic conductance that depends directly on voltage, not the ionic conductance itself. Therefore, in a voltage clamp experiment, if the voltage is changed quickly, the conductance has little chance to change, and the values of current and voltage just before and after the voltage step can be used to acquire two pairs of current and voltage measurements. If this procedure is repeated with the same starting voltage level and a range of second voltages, an *I–V* characteristic can be obtained.

As explained in more detail in Box 3.6, Hodgkin and Huxley obtained such *I–V* characteristics in squid giant axon and found that the quasi-ohmic *I–V* characteristics given in Equations 3.3–3.5 were appropriate for this membrane. They referred to this type of *I–V* characteristic as the **instantaneous *I–V* characteristic**, since the conductance is given no time to change between the voltage steps. In contrast, if the voltage clamp current is allowed time to reach a steady state after setting the voltage clamp holding potential, the *I–V* characteristic measured is called the **steady state *I–V* characteristic**. In contrast to the instantaneous *I–V* characteristic, this is non-linear in the squid giant axon. With the advent of single channel recording (Chapter 5), it is possible to measure the *I–V* characteristic of an open channel directly in the open and closed states, as for example do Schrempf *et al.* (1995).

A potentially more accurate way to model the *I–V* characteristics would be to use the GHK current equation (Box 2.4). For example, the sodium

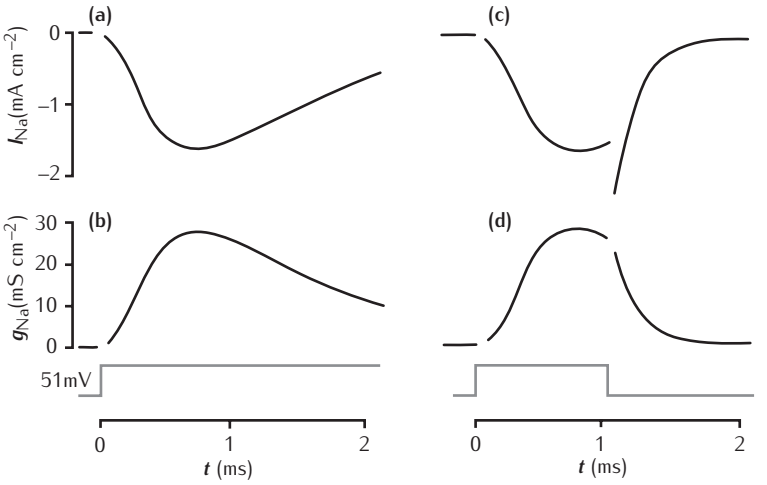

Fig. 3.16 Sodium current and sodium conductance under two different voltage clamp conditions. **(a)** The sodium current measured in response to a voltage clamp step at $t = 0$ of 51 mV above resting potential. **(b)** The conductance calculated from the current using Equation 3.3. **(c)** The current measured in response to a voltage step of the same amplitude, but which only lasted for 1.1 ms before returning to resting potential. The current is discontinuous at the end of the voltage step. The gap in the record is due to the capacitive surge being filtered out. **(d)** The conductance calculated from recording **(c)** and the value of the membrane potential. Although there is still a gap in the curve due to the capacitive surge, the conductance appears to be continuous at the point where the current was discontinuous. Adapted from Hodgkin and Huxley (1952b), with permission from John Wiley & Sons Ltd.

current would be given by:

$$I_{Na}(t) = \rho_{Na}(t)\,\frac{F^2V(t)}{RT}\left(\frac{[Na^+]_{in} - [Na^+]_{out}e^{-FV(t)/RT}}{1 - e^{-FV(t)/RT}}\right), \qquad (3.24)$$

where $\rho_{Na}(t)$ is the permeability to sodium at time t. This equation could be rearranged to determine the permeability over time from voltage clamp recordings, and then a gating particle model for the permeability (for example, of the form $\rho_{Na} = \bar{\rho}_{Na}m^3h$) could be derived. Sometimes it is desirable to use this form of the model, particularly where the I–V characteristic is non-linear and better fitted by the GHK equation. This is particularly the case for ions whose concentration differences across the membrane are large, such as in the case of calcium (Figure 2.11b).

The independence of gating particles

Alternative interpretations and fits of the voltage clamp data have been proposed. For example, Hoyt (1963, 1968) suggested that activation and inactivation are coupled. This was later confirmed through experiments that removed the inactivation in squid giant axon using the enzyme pronase (Bezanilla and Armstrong, 1977). Subsequent isolation of the inactivation time course revealed a lag in its onset that did not conform to the independent particle hypothesis. Inactivation now appears to be voltage *independent* and coupled to sodium activation. Consequently, more accurate models of sodium activation and inactivation require a more complex set of coupled equations (Goldman and Schauf, 1972). Unrestricted kinetic schemes, described in Section 5.5.3, provide a way to model dependencies such as this.

Gating current is not considered

In the HH model, the only currents supposed to flow across the membrane are the ionic currents. However, there is another source of current across the membrane, the movement of charges in channel proteins as they open and close. This **gating current**, described in more detail in Section 5.3.4, is very small in comparison to the ionic currents, so small in fact that it took

Box 3.6 Verifying the quasi-ohmic *I–V* characteristic

To verify that the instantaneous *I–V* characteristics of the sodium and potassium currents were quasi-ohmic, Hodgkin and Huxley (1952a) made a series of recordings using a two-step voltage clamp protocol. In every recording, the first step was of the same duration, and depolarised the membrane to the same level. This caused sodium and potassium channels to open. The second step was to a different voltage in each experiment in the series. The ion substitution method allowed the sodium and potassium currents to be separated.

Figure 3.16c shows one such recording of the sodium current. At the end of the step, the current increases discontinuously and then decays to zero. There is a small gap due to the capacitive surge. The current just after the discontinuous leap (I_2) depends on the voltage of the second step (V_2). When I_2 was plotted against V_2, a linear relationship passing through the sodium equilibrium potential E_{Na} was seen. The gradient of the straight line was the conductance at the time of the start of the second voltage step.

This justified the calculation of the conductance from the current and driving force according to Equation 3.3. Figure 3.16d shows the conductance so calculated. In contrast to the current, it is continuous at the end of the voltage step, apart from the gap due to the capacitive surge.

many years to be able to measure it in isolation from the ionic currents. Adding it to the HH model would make very little difference to the model's behaviour, and would not change the explanation provided by the model for the action potential. However, the gating current can be used to probe the detailed kinetics of ion channels. Thus, ignoring the gating current is a good example of a kind of simplification that is appropriate for one question, but if asking a different question, may be something to model with great accuracy.

3.5.2 Fitting the Hodgkin–Huxley formalism to data

The Hodgkin–Huxley formalism for a channel comprises

(1) an instantaneous *I–V* characteristic, e.g. quasi-ohmic or GHK equation;
(2) one or more gating variables (such as m and h) and the powers to which those gating variables are raised;
(3) expressions for the forward and backward rate coefficients for these variables as a function of voltage.

The data required for all the quantities are voltage clamp recordings using various protocols of holding potential of the current passing through the channel type in question. This requires that the channel be isolated by some method, such as the ion substitution method (Box 3.2), channel blockers, Section 5.3.2, or expression in oocytes, Section 5.3.3. The data required for each is now discussed.

Linear *I–V* characteristic

For greatest accuracy, the instantaneous *I–V* characteristic should be measured. Even the GHK equation might not be able to capture some features of the characteristic. Also, the reversal potential may differ significantly from the equilibrium potential of the dominant permeant ion if there are other ions to which the channel is significantly permeable. However, in practice, the quasi-ohmic approximation is often used with a measured reversal potential as equilibrium potential. When the intracellular and extracellular concentration differences are great, such as in the case of calcium, the GHK equation may be used.

Gating variables

If the channel displays no inactivation, only one gating variable is required, but if there is inactivation, an extra variable will be needed. The gating variable is raised to the power of the number of activation particles needed to capture the inflection in conductance activation, which then determines the voltage-dependent rate coefficient functions α_n, β_n of Equation 3.7.

Coefficients for each gating variable

The voltage dependence of the forward and backward reaction coefficients α and β for each gating particle need to be determined. The basis for this is the data from voltage clamp experiments with different holding potentials.

These can be obtained using the types of methods described in this chapter to determine plots of steady state activation and inactivation and time constants against voltage. With modern parameter estimation techniques (Section 4.5), it is sometimes possible to short circuit these methods. Instead, the parameters of a model can be adjusted to make the behaviour of the model as similar as possible to recordings under voltage clamp conditions.

The steady state variables, for instance n_∞ and τ_n in the case of potassium, need not be converted into rate coefficients such as α_n and β_n, since the kinetics of the gating variable can be specified using n_∞ and τ_n (Equation 3.11). This approach is taken, for example, by Connor *et al.* (1977) in their model of the A-type potassium current (Box 5.2). Hodgkin and Huxley fit smooth functions to their data points, but some modellers (Connor and Stevens, 1971c) connect their data points with straight lines in order to make a piecewise linear approximation of the underlying function.

If functions are to be fitted, the question arises of what form they should take. The functions used by Hodgkin and Huxley (1952d) took three different forms, each of which corresponds to a model of how the gating particles moved in the membrane (Section 5.8.3). From the point of view of modelling the behaviour of the membrane potential at a particular temperature, it does not really matter which two quantities are fitted to data or what functional forms are used, as long as they describe the data well. However, from the point of view of understanding the biophysics of channels, more physically principled fitting functions (Section 5.8) are better than arbitrary functions. This can include temperature dependence, rather than having to bolt this on using the value of Q_{10}.

3.6 Summary

In their model, Hodgkin and Huxley introduced active elements into the passive membrane equation. These active currents are specified through the concept of membrane-bound gated channels, or gates, each gate comprising a number of independent gating particles. While the Hodgkin–Huxley formalism does not relate directly to the physical structure of channels, it does provide a framework within which to describe experimental data. In particular, the use of kinetic reaction equations allows the system to be fitted to voltage-dependent characteristics of the active membrane currents through the voltage dependence of the kinetic rate coefficients. Putative functions for the kinetic rate coefficients are fitted to experimental voltage clamp data. The resulting quantitative model not only replicates the voltage clamp experiments to which it is tuned, but also reproduces the main features of the action potential.

In this chapter we have been considering the squid giant axon only. Furthermore, we have focused on single stretches of axon and have not included features such as branch points, varicosities and axon tapering in the model. These extensions may be added to the models using the multicompartmental model approach. As seen previously, a single equivalent electrical circuit representing an isopotential patch of membrane can be connected to other membrane circuits in various ways to form an approximation of membrane area and discontinuities. This approach is introduced and discussed in Chapter 4.

Representing more complex neurons requires a model to contain more than sodium and potassium conductances. This can be achieved by including in the equivalent electrical circuit any number of transmembrane conductances in series with a voltage source representing new ionic currents. The voltage dependence of conductances may be characterised by the Hodgkin–Huxley formalism if the independent gating particle approach is deemed accurate enough. However, as will be seen in Chapter 5, the Hodgkin–Huxley formalism cannot explain some behaviours of ion channels, and more complex models are required. Conductances may also exhibit more than voltage dependence; for example, ligand-gated channels and channels dependent on ionic concentrations. These variations are discussed in Chapters 5 and 7.